# Wrong-Way Behavior of Packed-Bed Reactors: Influence of Reactant Adsorption on Support

**Andrew Il'in and Dan Luss**
Dept. of Chemical Engineering, University of Houston, Houston, TX 77204

*Wrong-way behavior refers to a large transient temperature increase caused by a sudden reduction in the feed temperature or increase in the feed rate to a packed-bed reactor operating at an intermediate or high level of conversion. This dynamic temperature rise may be affected by reactant adsorption on the inert catalyst support. The wrong-way behavior usually leads to formation of a downstream-moving temperature front. In such cases, reactant adsorption tends to moderate and decrease the maximal transient temperature of these fronts. However, when the wrong-way behavior generates an upstream-moving temperature front, reactant adsorption may substantially increase the temperature rise over that attained in its absence and ignite the reactor. Reactant adsorption may also lead to surprising dynamic effects upon changes in feed velocity.*

## Introduction

The difference in the propagation speed of concentration and temperature disturbances in a packed-bed reactor leads to a surprising dynamic feature, namely the wrong-way behavior. This feature refers to a transient temperature rise induced by a sudden reduction in the feed temperature or an increase in the velocity. It occurs because a sudden change in the feed temperature decreases the conversion in the upstream section of the reactor; consequently, the still-hot catalyst in the downstream section is exposed to a higher reactant concentration than under the original steady-state operation, leading to an increase in the rate of heat generation by the reaction. The wrong-way behavior may be considered to be the distributed parameter analog of the inverse response encountered in lumped-parameter systems.

The first theoretical prediction of the wrong-way behavior was made by Matros and Beskov (1965), Boreskov et al. (1965), and Crider and Foss (1966). It was observed by Hoiberg et al. (1971), Van Doesburg and DeJong (1976a,b), and Sharma and Hughes (1979a,b). A simple, conservative estimate of the wrong-way behavior was presented by Mehta et al. (1981). More accurate predictions were presented by Pinjala et al. (1988) and Chen and Luss (1989), who used a two-phase model accounting for axial dispersion of heat and mass. These analyses predicted that in certain cases the wrong-way behavior may ignite a reactor and shift it permanently to an undesired high-temperature steady state. An experimental finding of such a behavior was reported by Sharma and Hughes (1979b). The impact of the wrong-way behavior on the temperature excursions in an automobile convertor was studied by Oh and Cavendish (1982).

In many catalytic processes, a rather large amount of the reactants and/or products may adsorb on the inert support. This process usually does not affect the steady-state operation of the reactor. However, it may have an important impact on the dynamic features of the reactor. For example, reactant adsorption on the support may delay and moderate the impact of a transient change in reactant concentration. On the other hand, a transient local-temperature increase may release adsorbed reactant, increasing further the magnitude of the temperature perturbation. Previous studies of wrong-way behavior did not consider the potential impact of reactant adsorption on the inert support. The goal of this study is to assess the impact of this process.

## Mathematical Model

The packed-bed reactor is described by a two-phase model, which accounts for the interfacial transport resistances between the fluid and the catalytic pellets and the axial dispersion of species and heat. The temperature gradient within the pellets is usually small relative to the interfacial gradient (Carberry, 1975) and is ignored. In addition, we ignore any intraparticle concentration gradients of the reactants within the catalyst pores and on the surface of the inert support.

We assume that a single, first-order, irreversible reaction occurs in the reactor and that the reactant is adsorbed also on the inert support. The reaction occurs on the supported catalytic sites and the net rate of adsorption of the reactant on the inert support satisfies the relation:

$$R_a(C_p, C_s, T_s) = k_a(T_s)C_p\left(1-\frac{C_s}{Q_s}\right) - k_d(T_s)\frac{C_s}{Q_s}, \quad (1)$$

where $C_p$ and $C_s$ are reactant concentration within the pores of the pellet and on the inert support, respectively; $Q_s$ is the saturation concentration on the support; and $k_a$ and $k_d$ are the adsorption and desorption rate constants and have the following temperature dependence:

$$k_a(T_s) = k_a(T_r)\exp\left[\frac{E_a}{R_g}\left(\frac{1}{T_r}-\frac{1}{T_s}\right)\right], \quad (2)$$

$$k_d(T_s) = k_d(T_r)\exp\left[\frac{E_d}{R_g}\left(\frac{1}{T_r}-\frac{1}{T_s}\right)\right], \quad (3)$$

We select the reference temperature $T_r$ so that $k(T_r) = u/L$. The mathematical model of the reactor consists of the following dimensionless species and energy balances:

$$\frac{1}{Le}\frac{\partial x}{\partial t} + M(x-x_p) = \frac{1}{Pe_m}\frac{\partial^2 x}{\partial z^2} - \frac{\partial x}{\partial z}, \quad (4)$$

$$\frac{1}{Le}\frac{\partial y}{\partial t} + H(y-y_s) + U(y-y_w) = \frac{1}{Pe_h}\frac{\partial^2 y}{\partial z^2} - \frac{\partial y}{\partial z}, \quad (5)$$

$$\frac{1}{Le^*}\frac{\partial x_p}{\partial t} = M(x-x_p) - r_a(x_p, x_s, y_s) - x_p X(y_s), \quad (6)$$

$$\left(1-\frac{1}{Le}\right)\frac{\partial y_s}{\partial t} = H(y-y_s) + \beta x_p X(y_s) + \beta_a r_a(x_p, x_s, y_s), \quad (7)$$

$$\frac{R}{Le^*}\frac{\partial x_s}{\partial t} = r_a(x_p, x_s, y_s), \quad (8)$$

where

$$X(y_s) = \exp\left(\frac{1}{y_r}-\frac{1}{y_s}\right), \quad (9)$$

$$r_a(x_p, x_s, y_s) = D_a x_p X(y_s)^{\sigma_a}(1-x_s) - D_d X(y_s)^{\sigma_d} x_s. \quad (10)$$

The dimensionless groups are defined as:

$$x=\frac{C}{C_f},\ x_p=\frac{C_p}{C_f},\ x_s=\frac{C_s}{Q_s},\ y=\frac{R_gT}{E},$$

$$y_s=\frac{R_gT_s}{E},\ y_r=\frac{R_gT_r}{E},\ y_w=\frac{R_gT_w}{E},$$

$$Pe_h=\frac{L\,u\,\rho_f c_f}{\lambda},\ Pe_m=\frac{L\,u}{D},\ Le=1+\frac{(1-\epsilon)\rho_s c_s}{\epsilon\,\rho_f c_f},\ Le^*=\frac{\epsilon\,Le}{(1-\epsilon)}$$

$$H=\frac{3\,h\,L(1-\epsilon)}{u\,r_p\rho_f c_f},\ M=\frac{3\,k_c L(1-\epsilon)}{u\,r_p},$$

$$U=\frac{2\,h_w L}{u\,r\,\rho_f c_f},\ \beta=\frac{R_g}{E}\frac{(-\Delta H)C_f}{\rho_f c_f},$$

$$D_a=\frac{k_a(T_r)L(1-\epsilon)S_g\rho_s}{u},\ D_d=D_a\frac{k_d(T_r)}{k_a(T_r)C_f},\ \beta_a=\beta\frac{(-\Delta H_a)}{(-\Delta H)},$$

$$R=\frac{S_g\rho_s Q_s}{C_f},\ \sigma_a=\frac{E_a}{E},\ \sigma_d=\frac{E_d}{E},\ t=\left(\frac{u\,t'}{\epsilon L}\right)\frac{1}{Le},\ z=\frac{z'}{L}. \quad (11)$$

The corresponding boundary conditions are:

$$1-x = -\frac{1}{Pe_m}\frac{\partial x}{\partial z},\quad z=0, \quad (12)$$

$$y-y_f = \frac{1}{Pe_h}\frac{\partial y}{\partial z},\quad z=0, \quad (13)$$

$$\frac{\partial x}{\partial z}=\frac{\partial y}{\partial z}=0,\quad z=1. \quad (14)$$

The initial conditions of all the state variables correspond to a steady state with a specified feed temperature $y_{f1}$. At $t=0$, the feed temperature is suddenly reduced to a new value of $y_{f2}$.

The mathematical model, Eqs. 4-8, consists of two partial differential equations, Eqs. 4-5, with small parameters multiplying the highest-order derivatives and three nonlinear ordinary differential equations. An implicit finite differences integration scheme with nonequal space and time-step size was used in the numerical simulations. The axial derivatives were approximated by (Drobyshevich and Il'in, 1981):

$$\frac{1}{Pe_m}\frac{\partial^2 x}{\partial z^2} - \frac{\partial x}{\partial z} = \frac{2}{(h_{i-1}+h_i)}\times\left[\frac{x_{i-1,j}}{1-\exp(-Pe_m h_{i-1})} - \frac{x_{ij}}{\exp(Pe_m h_{i-1})-1} - \frac{x_{ij}}{1-\exp(-Pe_m h_i)} + \frac{x_{i+1,j}}{\exp(Pe_m h_i)-1}\right] + O[\max(h_i)] \quad (15)$$

$$\left(x-\frac{1}{Pe_m}\frac{\partial x}{\partial z}\right)_{z=0} = \frac{x_{0j}}{[1-\exp(-Pe_m h_0)]} - \frac{x_{1j}}{[\exp(Pe_m h_0)-1]} + O(h_0) \quad (16)$$

$$\left(\frac{\partial x}{\partial z}\right)_{z=1} = \frac{x_{Nj}-x_{N-1,j}}{h_{N-1}} + O(h_{N-1}). \quad (17)$$

This approximation for $x$ was applied to $y$ as well. The basis for this approximation is described in Appendix 1. Here, $i$ is the number of spatial grid-point, (0, 1, ...$N$), $j$ the number of the time grid-point, and $h_i$ the step size $(z_{i+1}-z_i)$. The difference between the grid-points was adjusted according to the stiffness of the solution. An additional grid-point is placed in the center of the step, when

$$|x_{i+1,j}-x_{i,j}| > \epsilon_{\max}, \quad (18)$$

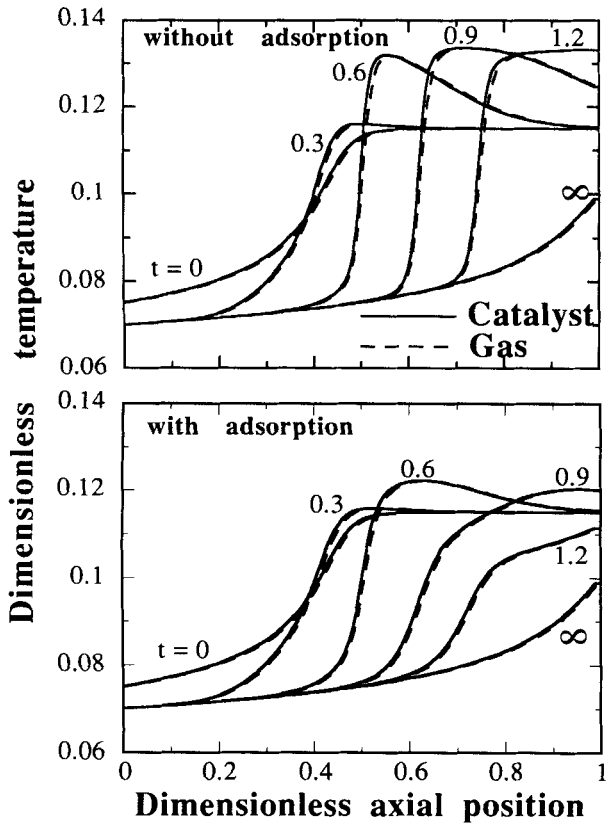


**Figure 1. Transient temperature profiles following a sudden reduction in the dimensionless feed temperature in an adiabatic reactor from 0.075 to 0.07 for a case with and without reactant adsorption on the support.**

$Pe_m = 1{,}000$, $Pe_h = 250$, $\beta = 0.04$, $y_r = 0.08$. For the adsorption case, $D_a = 20.0$, $D_d = 1.0$.

for one of the variables. The values at this point are determined by spline interpolation (Gayevoy and Chumakova, 1980). When

$$|x_{i-1,j} - x_{i,j}| < \epsilon_{\min} \quad \text{and} \quad |x_{i+1,j} - x_{i,j}| < \epsilon_{\min}, \tag{19}$$

a grid point is deleted in the next step. (We used $\epsilon_{\max} = 3 \times 10^{-2}$ and $\epsilon_{\min} = 10^{-2}$.) The finite-difference solution is iterated until all the variables satisfy

$$|x_{i,j}^n - x_{i,j}^{n-1}| < \epsilon_t \tag{20}$$

where $n$ is the iteration number. When $n$ exceeds 10, $\Delta t_j$ is decreased by a factor of 2; if $n$ is smaller than 3, $\Delta t_j$ is increased by 1%. Numerical simulations with different step sizes and $\epsilon_t$ values indicated that the numerical procedure led to a high accuracy. We used $\epsilon_t = 10^{-6}$.

## Influence of Feed Temperature Reduction

Extensive numerical calculations were carried out to determine the impact of reactant adsorption on the inert support on the magnitude and features of the temperature excursion caused by the wrong-way behavior. In all the simulations reported here, we assumed that $Le = 100$, $M = H = 180$, $U = 2$,

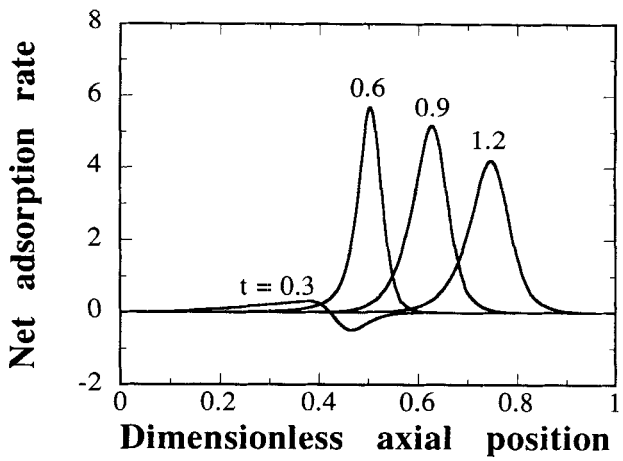


**Figure 2. Transient reactant-adsorption rate for the case in Figure 1 (bottom).**

$R = 100$, $\sigma_a = 0.15$, $\sigma_d = 0.5$, and $\beta_a = 0.014$. The values of the remaining parameters are specified at each figure. A set of values of actual parameters giving rise to the dimensionless parameter values used in Figures 6–10 and 13 is reported in Appendix 2. It was found that when the reactor has a unique steady state, reactant adsorption tends to reduce the magnitude of the transient temperature-rise following a sudden decrease in feed temperature. For example, Figure 1 compares temperature profiles in an adiabatic packed-bed reactor following a sudden decrease in the feed temperature. The maximal transient temperature rise, $\max(y_s)$, for the case that the reactant does not adsorb on the support (Figure 1, top), is higher than that when the reactant adsorbs on the inert support. Without adsorption, the peak solid temperature ($y_s = 0.134$) exceeds the maximal steady-state temperature by 48% of the adiabatic temperature rise ($\beta = 0.04$), while with adsorption the maximal solid temperature excursion ($y_s = 0.122$) exceeds the adiabatic temperature rise by only 19%.

The reason for the difference is that the support tends to adsorb the reactant during the transient period, reducing the reactant concentration and rate of heat release at the hot spot. The transient feed-temperature reduction leads to two opposing effects. In the upstream section of the reactor, the cooling increases the reactant concentration and hence the rate of reactant adsorption. This adsorption reduces the transient downstream reactant concentration. Next to the hot spot, the temperature rise enhances reactant desorption increasing the reaction rate. The simulations show that under practical conditions the first effect is the dominant one, decreasing the transient reaction rate at the hot spot. Hence, the transient peak-temperature is decreased by the reactant adsorption. Profiles of the transient adsorption rate (Figure 2) for the case shown in Figure 1 (bottom) show that a net rate of adsorption occurs practically everywhere in the reactor during the transient period. Initially the adsorbed reactant concentration is high at the upstream section of the reactor. Adsorption occurs only after some time as the temperature wave reaches the section of the reactor in which the initial concentration of adsorbed reactant is not high. The simulation (Figure 1) indicates that the adsorption shortened somewhat the duration of the transient period: that is, the temperature-waves move at a slightly higher velocity.

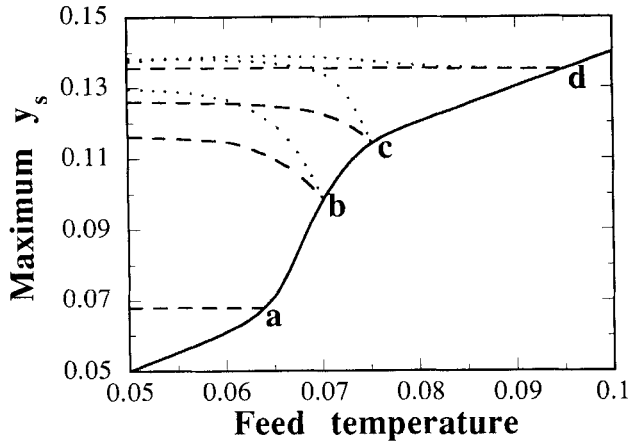


**Figure 3. Dependence of the maximal catalyst transient temperature on the original (solid line) and the new feed temperature for cases with no adsorption (dotted line) and with reactant adsorption (dashed line).**

The impact of adsorption is illustrated by the master diagram, Figure 3, which describes the dependence of the maximal transient temperature for cases with (dashed line) and without reactant adsorption (dotted line) on the initial (solid line) and

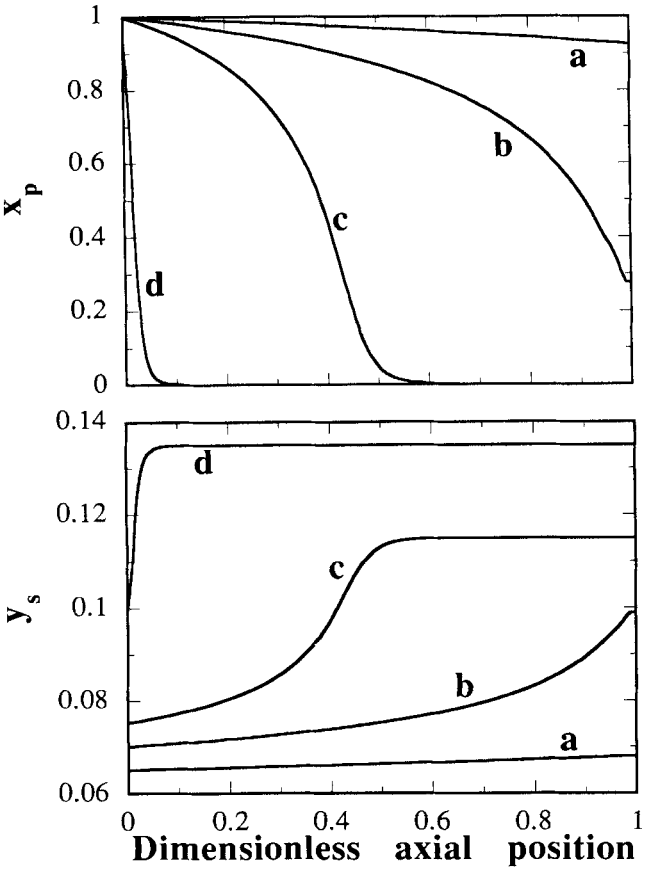


**Figure 4. Dimensionless initial steady-state catalyst concentration and temperature for the four cases in Figure 3.**

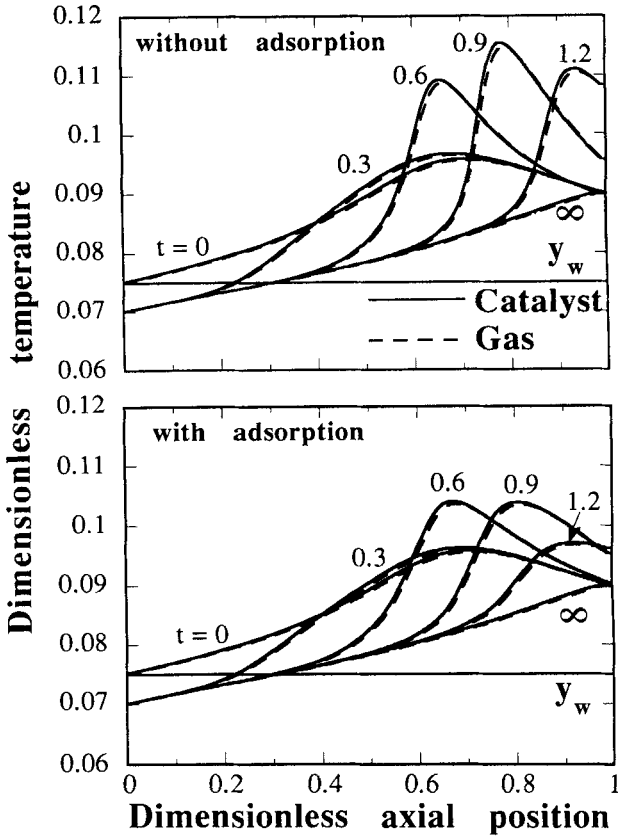


**Figure 5. Transient temperature profiles following a sudden reduction in the dimensionless feed temperature in a cooled reactor from 0.075 to 0.07.**

Same parameters as in Figure 1 and $y_w = 0.07$.

new feed-temperature for four cases. Each dotted or dashed line describes the maximal transient temperature vs. new feed temperature for a specific feed temperature (intersection of solid and dotted or dashed lines). As already shown by Pinjala et al. (1988) and Chen and Luss (1989), an appreciable transient temperature rise occurs only for the cases with intermediate or high conversions, but for which the steady-state temperature front is not right at the reactor inlet, for example, at points b and c, but not at points a or d in Figure 3. (The steady-state profiles corresponding to these four cases are shown in Figure 4.) The computations show that adsorption on the support reduced the transient temperature rise in this case for all new feed-temperature values.

The influence of reactant adsorption on the inert support on the wrong-way behavior in a cooled reactor is similar to that in an adiabatic reactor: it reduces the peak temperature rise when the temperature front moves in the downstream direction. For example, Figure 5 (top) shows a case in which a feed-temperature reduction generates a transient solid-temperature peak ($y_s = 0.116$) exceeding by 96% the original steady-state temperature rise. In the presence of reactant adsorption (Figure 5, bottom), the maximal transient-temperature increase ($y_s = 0.106$) is only 48% of the original steady-state temperature rise.

When the reactor may have different steady states and the

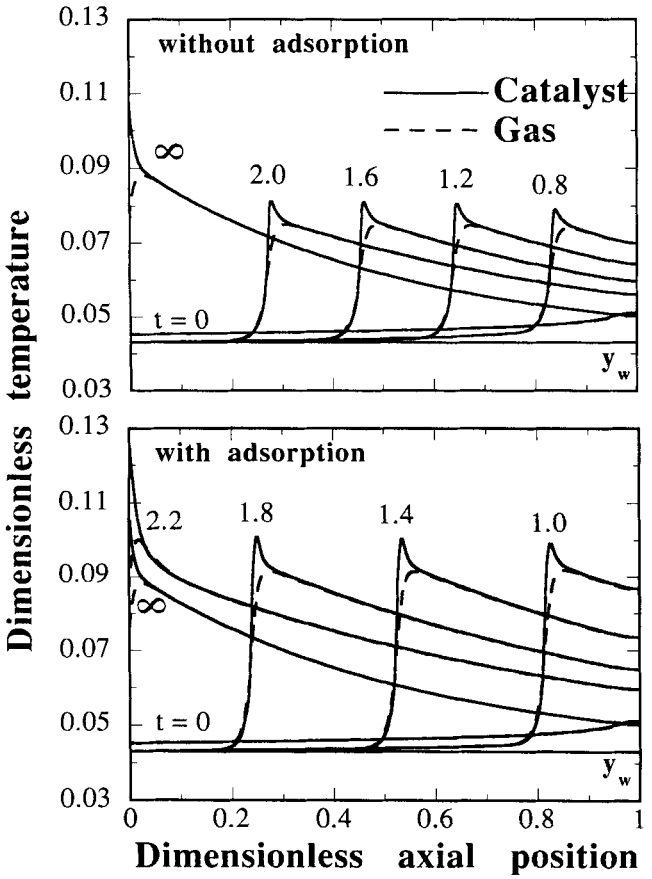


**Figure 6. Transient temperature profiles following a sudden reduction of the dimensionless feed temperature for a cooled reactor from 0.04513 to 0.043 for cases with and without reactant adsorption.**

$Pe_h = 50$, $Pe_m = 200$, $y_w = 0.043$, $\beta = 0.05$, $\gamma_r = 0.05$. For the adsorption case, $D_a = 20.0$, $D_d = 1.0$.

initial steady state is on the extinguished branch close to the ignition point, the wrong-way behavior may generate transient, backward-moving temperature fronts. In such cases, reactant adsorption on the support may significantly increase the transient peak temperature caused by the wrong-way behavior. A typical example is shown in Figure 6. Here, a sudden reduction in the feed temperature from 0.04513 to 0.043 causes a backward propagation of a temperature front and ignition of the reactor, which is similar to the behavior found by Pinjala et al. (1988) and Chen and Luss (1989). When the reactant is not adsorbed on the support (Figure 6, top), the maximal transient gas and solid peak temperatures do not exceed those of the new ignited steady state ($t = \infty$). On the other hand, when the reactant is adsorbed on the support (Figure 6, bottom), the transient peak temperature may exceed that of the new steady state. For example, at $t = 2.2$, the transient catalyst temperature (0.128) exceeds that of the new peak steady-state temperature by 31% of the maximal steady-state temperature difference between the hot spot and the feed. Similarly, the maximal transient gas temperature (0.101) exceeds that of the steady state (0.088). The reason for different behaviors is that the backward-moving temperature front desorbs a large amount

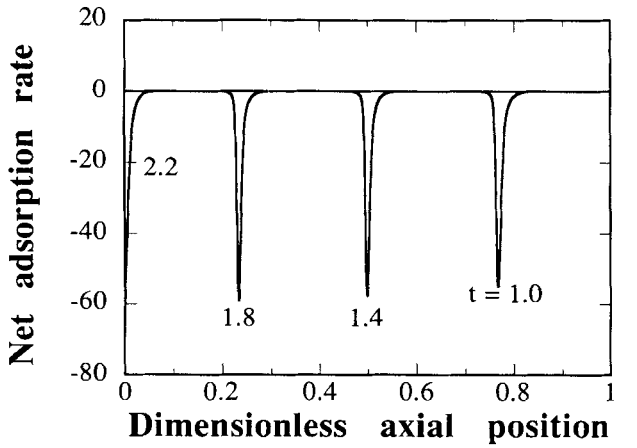


**Figure 7. Profiles of transient net adsorption rate on the support for the case in Figure 6 (bottom).**

of the reactant (Figure 7), which increases the peak transient temperature. Similar to the case of forward-moving fronts, the adsorption increases also in this case the velocity of the moving temperature fronts. (Compare the top and bottom of Figure 6.)

Reactant adsorption tends in general to sharpen the temperature fronts in the solid phase. This is illustrated in Figure 6. This sharpening of the temperature front is associated with a rather high rate of desorption at the front. This feature becomes more pronounced for higher activation energy of the reaction.

The behavior of the system is best understood by inspection of the master diagram, Figure 8, which describes both the steady state of the system (solid line) and the maximal transient temperature as a function of the new feed temperature for the initial steady state shown in Figure 6: $y_{f1} = 0.04513$. In this case, multiple steady states exist for all feed temperatures $0 < y_f < y_{f1}$.

When the reactants do not adsorb on the support and the initial feed temperature is close to ignition, a feed temperature

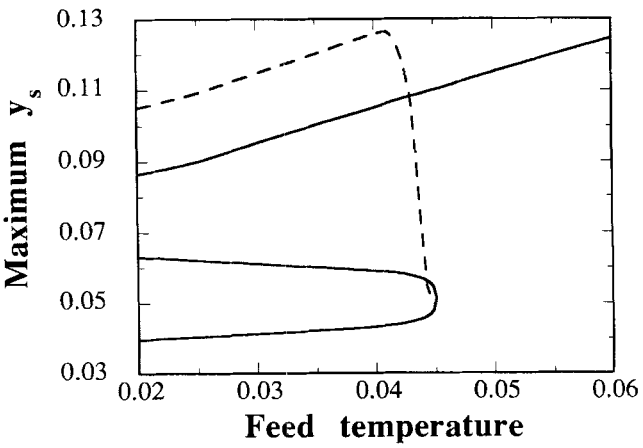


**Figure 8. Dependence of the maximal transient temperature on the new feed temperature for the case with adsorption (dashed line).**

Steady states are shown by solid line. Initial feed temperature, 0.04513. Parameters same as in Figure 6.

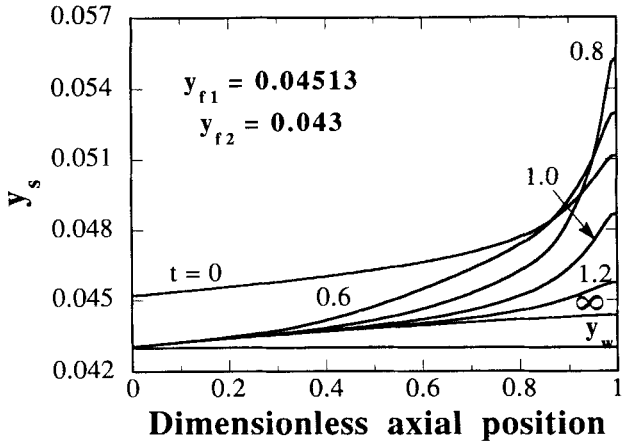


**Figure 9. Transient temperature profiles following a sudden reduction of the dimensionless feed temperature for the same parameters as in Figure 6 except for $D_a = 24.0$ and $D_d = 1.2$.**

decrease causes the reactor to ignite and to shift to the newly ignited steady state. The maximal transient peak temperature never exceeds that of the ignited state. Figure 8 shows the transient peak temperatures obtained when the reactant is adsorbed on the support. In this case, the maximal transient temperature may significantly exceed that obtained when the reactant is not adsorbed.

The adsorption rate constant has a very important impact on the dynamic behavior when a backward-moving temperature front is formed. When the reactant-adsorption rate constant is very high (Figure 9), its adsorption at the downstream section of the reactor may reduce the transient temperature rise so that ignition will not occur (Figure 9) even though it would ignite for a lower adsorption rate constant or in the absence of reactant adsorption. This point is illustrated again in Figure 10, which describes the dependence of the maximal transient gas peak temperature on the adsorption rate constant. For small values of the adsorption rate constant, or equivalently of $D_a$, the maximal transient temperature rise increases

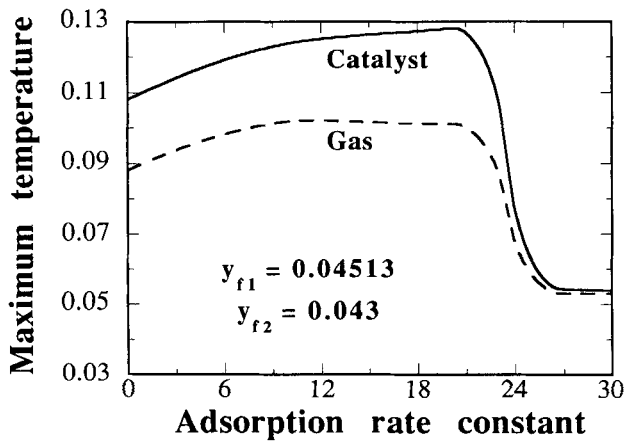


**Figure 10. Dependence of the maximal transient temperature on the adsorption rate constant with $D_a/D_d = 20.0$.**

Other parameters are the same as in Figure 6.

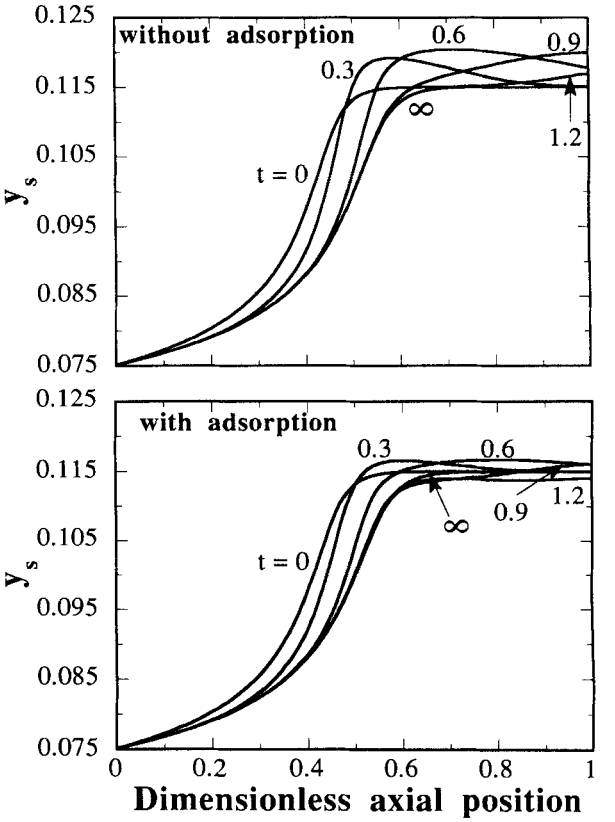


**Figure 11. Wrong-way behavior caused by a 20% increase in feed temperature.**

Parameter values same as in Figure 1.

with increasing $D_a$. However, for $D_a$ values larger than 23, increasing the adsorption rate constant reduces the maximal temperature rise. For $D_a$ larger than 23.5, the transient temperature rise is much smaller than that attained in the absence of reactant adsorption ($D_a = 0$).

### *Influence of Feed Rate Perturbations*

The discussion above was of a wrong-way behavior caused by a sudden reduction in the feed temperature. However, it may also be caused by variation in the velocity. Specifically, a sudden increase in the velocity, which shifts the temperature profile in the downstream direction, may lead to a transient temperature rise.

The linear velocity affects the values of six parameters in the steady-state model, namely, $y_r$, $Pe_m$, $Pe_h$, $H$, $M$, and $U$. The last five depend rather weakly on small velocity variations. In our numerical simulations, we accounted only for the impact of the velocity variations on $y_r$, the value of which has a strong impact on the steady-state profile. In addition, we accounted for the impact of velocity on $t$, $D_a$, and $D_d$.

Figure 11 (top) describes a wrong-way behavior caused by a 20% increase in the linear velocity. The maximal transient temperature ($y_s = 0.1204$) exceeds the adiabatic temperature rise by 15% for the case in which no adsorption occurs. A decrease in the velocity shifts the temperature profile in the upstream direction, but does not cause any transient temperature increase (Figure 12, top).

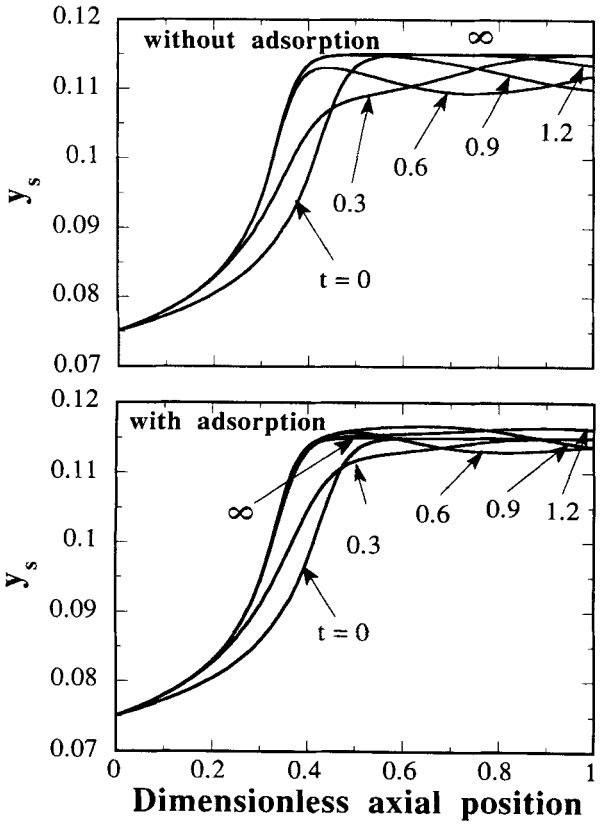


**Figure 12. Transient temperature profiles following a 20% reduction in feed velocity.**

Parameter values same as in Figure 1.

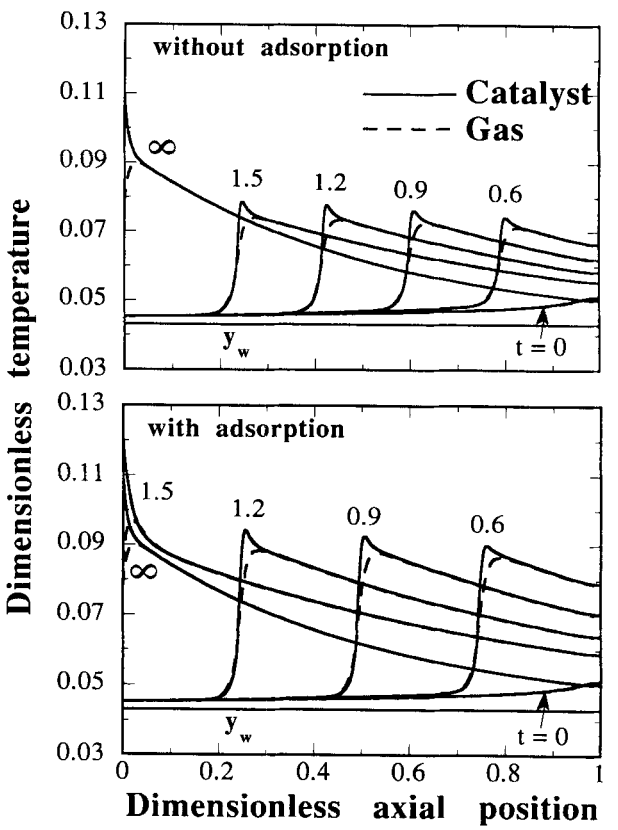


**Figure 13. Temperature profiles obtain as the reactor is ignited following a 10% decrease in the feed velocity.**

Parameter values same as in Figure 6.

When the reactant is adsorbed on the support, a wrong-way behavior is again observed upon an increase in the velocity (Figure 11, bottom). However, the reactant adsorption moderates the maximal transient temperature, which is 4% of the adiabatic temperature rise, in contrast to 15% when the reactant is not adsorbed.

It is of interest to note that when reactant adsorption occurs, a transient temperature rise occurs even for a reduction in the feed velocity (Figure 12, bottom), while no such effect occurs without reactant adsorption. The reason is that the backward movement of the temperature front releases adsorbed reactant, and this increases temporarily the rate of the heat generation by the chemical reaction.

When multiple steady-state exists and the reactor operates close to the ignition point, an increase in the feed velocity does not lead to a wrong-way behavior, and the reactor remains on the low-temperature, low-conversion branch. However, a decrease in the feed velocity may lead to ignition. When no reactant adsorption exists, the maximal transient temperature does not exceed that of the ignited steady state (Figure 13, top). In the presence of adsorption, the maximal transient temperature may exceed that of the new steady state. For example, Figure 13 (bottom) describes a situation in which the maximal transient temperature of 0.1216 exceeds the new steady-state temperature rise by 18%. This behavior is again caused by the backwards movement of the temperature front and the accompanied reactant release.

## Conclusions

Reactant adsorption on the inert catalyst support tends to moderate and decrease the transient temperature rise caused by a wrong-way behavior when the transient temperature front moves in the downstream direction. This happens in most practical cases and in the important case in which each catalyst particle in the reactor has a unique steady state. When a highly exothermic reaction is carried out in a cooled reactor close to the extinction point, the wrong-way behavior may generate a backward-moving temperature front and lead to an undesired ignition of the reactor. This is usually accompanied by an effect that is not accounted for in our model: namely, the taking-over by an undesired reaction, the rate of which is negligible under the standard steady state. In such cases, reactant adsorption on the support may substantially increase the transient temperature rise over that occurring in its absence, leading to an undesired runaway.

Once a wrong-way behavior has started, one may quench it by replacing the reactant feed with an inert stream having a high heat capacity. When a large amount of reactant is adsorbed on the support, this control policy may be less effective as in the absence of adsorption.

## Acknowledgment

We wish to thank Thomas R. Keane for useful comments and suggestions.

## Notation

$c$ = specific heat
$C$ = concentration of reactant
$D$ = axial mass dispersion coefficient
$D_a$ = Damköhler number for adsorption, defined by Eq. 11
$D_d$ = Damköhler number for desorption, defined by Eq. 11
$E$ = activation energy
$h$ = interfacial heat-transfer coefficient
$h_i$ = space step size
$h_w$ = overall heat-transfer coefficient at wall
$H$ = dimensionless heat-transfer parameter, defined by Eq. 11
$(-\Delta H)$ = heat of reaction
$k(T_r)$, $k_a(T_r)$, $k_d(T_r)$ = reaction, adsorption and desorption rate constants at $T=T_r$
$k_c$ = interfacial mass-transfer coefficient
$L$ = reactor length
$Le$ = Lewis number, defined by Eq. 11
$Le^*$ = modified Lewis number, defined by Eq. 11
$M$ = dimensionless mass-transfer parameter, defined by Eq. 11
$Pe$ = Peclet number, defined by Eq. 11
$Q_s$ = saturation concentration of adsorbed reactant on support
$r$ = reactor radius
$r_a(x_p, x_s, y_s)$ = dimensionless adsorption rate, defined by Eq. 10
$r_p$ = particle radius
$R$ = coefficient, defined by Eq. 11
$R_a(C_p, C_s, T_s)$ = adsorption rate, defined by Eq. 1
$R_g$ = universal gas constant
$S_g$ = specific surface area
$t$ = dimensionless time, defined by Eq. 11
$t'$ = time
$\Delta t_j$ = time step size
$T$ = temperature
$T_r$ = reference temperature, defined by $k(T_r)=u/L$
$u$ = superficial velocity
$U$ = dimensionless heat-transfer parameter at wall, defined by Eq. 11
$x$ = dimensionless concentration, defined by Eq. 11
$X(y_s)$ = dimensionless rate function defined by Eq. 9
$y$ = dimensionless temperature defined by Eq. 11
$z$ = dimensionless axial position coordinate, defined by Eq. 11
$z'$ = axial position coordinate

### *Greek letters*

$\beta$ = dimensionless heat of reaction, defined by Eq. 11
$\beta_a$ = dimensionless heat of reaction, defined by Eq. 11
$\epsilon$ = void fraction of bed
$\epsilon_{max}$, $\epsilon_{min}$, $\epsilon_l$ = numerical method criteria, used in Eqs. 18, 19, and 20
$\lambda$ = axial heat dispersion coefficient
$\rho$ = density
$\sigma$ = activation energy ratio, defined by Eq. 11

### *Subscripts*

$a$ = adsorption
$d$ = desorption
$f$ = feed, fluid
$h$ = heat
$i$ = number of spatial grid-point
$j$ = number of temporal grid-point
$m$ = mass
$n$ = iteration number
$p$ = pellet, particle
$r$ = reference
$s$ = solid, support
$w$ = wall

## Literature Cited


Boreskov, G. K., and M. G. Slinko, "Modelling of Chemical Reactors," *Pure Appl. Chem.*, **10**, 611 (1965).

Carberry, J., "On the Relative Importance of External-Internal Temperature Gradients in Heterogeneous Catalysts," *Ind. Eng. Chem. Fund.*, **14**, 129 (1975).

Chen, Y. C., and D. Luss, "Wrong-Way Behavior of Packed-Bed Reactors: Influence of Interphase Transport," *AIChE J.*, **35**, 1148 (1989).

Crider, J. E., and A. S. Foss, "Computational Studies of Transients in Packed Tubular Chemical Reactors," *AIChE J.*, **12**, 514 (1966).

Drobyshevich, V. I., and V. P. Il'in, "Modelling of Heat- and Mass-Exchanger Processes in Reactors with a Fixed Catalyst Bed," Preprint **307**, Computer Center, Siberian Section, Acad. Sci. USSR, Novosibirsk (1981).

Gayevoy, V. P., and N. A. Chumakova, "On Nonstationary Net Method and Its Applications," *Math. Methods in Chemistry*, Moscow, CNIITEneftechim, **2**, 164 (1980).

Hoiberg, J. A., B. C. Lyche, and A. S. Foss, "Experimental Evaluation of Dynamic Models for a Fixed-Bed Catalytic Reactor," *AIChE J.*, **17**, 1434 (1971).

Liu, S. L., and N. R. Amundson, "Stability of Nonadiabatic Packed-Bed Reactors," *Ind. Eng. Chem. Fund.*, **2**, 12 (1963).

Marchuk, G. I., *Numerical Methods for Nuclear Reactor Calculations*, Consultants Bureau, New York (1959).

Matros, Y. S., and V. S. Beskov, "Calculation of Contact Apparatus with Internal Heat-Transfer as an Object of Control," *Khimicheskaya Promyshlennost.*, **5**, 357 (1965).

Mehta, P. S., W. N. Sams, and D. Luss, "Wrong-Way Behavior of Packed-Bed Reactors: I. The Pseudo-Homogeneous Model," *AIChE J.*, **27**, 234 (1981).

Oh, S. H., and J. C. Cavendish, "Transients of Monolithic Catalytic Convertors: Response to Step-Changes in Feedstream Temperature as Related to Controlling Automobile Emissions," *I.E.C. Proc. Des. Dev.*, **21**, 29 (1982).

Pinjala, V., Y. C. Chen, and D. Luss, "Wrong-Way Behavior of Packed-Bed Reactors: II. Impact of Thermal Diffusion," *AIChE J.*, **34**, 1663 (1988).

Sharma, C. S., and R. Hughes, "The Behavior of an Adiabatic Fixed-Bed Reactor for the Oxidation of Carbon Monoxide: I. General Parametric Studies," *Chem. Eng. Sci.*, **34**, 613 (1979a).

Sharma, C. S., and R. Hughes, "The Behavior of an Adiabatic Fixed-Bed Reactor for the Oxidation of Carbon Monoxide: II. Effect of Perturbations," *Chem. Eng. Sci.*, **34**, 625 (1979b).

Van Doesburg, H., and W. A. DeJong, "Transient Behavior of an Adiabatic Fixed-Bed Methanator: I. Experiments with Binary Feeds of CO or $CO_2$ in Hydrogen," *Chem. Eng. Sci.*, **31**, 45 (1976a).

Van Doesburg, H., and W. A. DeJong, "Transient Behavior of an Adiabatic Fixed-Bed Methanator: II. Methanation of Mixtures of Carbon Monoxide and Carbon Dioxide," *Chem. Eng. Sci.*, **31**, 53 (1976b).


## Appendix 1: Derivation of Eqs. 15 and 16

We outline the procedure developed by Drobyshevich and Il'in (1981) extending the method of Marchuk (1959).

We define:

$$\Phi(z)=\frac{1}{Pe_m}\frac{\partial x}{\partial z}-x=\frac{\exp(Pe_m z)}{Pe_m}\frac{\partial}{\partial z}[\exp(-Pe_m z)x]. \quad \text{(A1)}$$

Integrating Eq. 4 from $z_{i-1/2}$ to $z$ we get:

$$\Phi(z_{i-1/2}) = \Phi(z) - \int_{z_{i-1/2}}^{z} \left[ \frac{1}{Le} \frac{\partial x}{\partial t} + M(x - x_p) \right] dz. \quad \text{(A2)}$$

Multiplying Eq. A2 by $\exp(-Pe_m z)$ and integrating from $z_{i-1}$ to $z_i$, using Eq. A1, gives:

$$\frac{[\exp(-Pe_m z_{i-1}) - \exp(-Pe_m z_i)]}{Pe_m} \Phi(z_{i-1/2}) = \frac{\exp(-Pe_m z_i)x(z_i) - \exp(-Pe_m z_{i-1})x(z_{i-1})}{Pe_m} - \int_{z_{i-1}}^{z_i} \exp(-Pe_m z) dz' \int_{z_{i-1/2}}^{z'} \left( \frac{1}{Le} \frac{\partial x}{\partial t} + M(x - x_p) \right) dz. \quad \text{(A3)}$$

Equation A3 may be rewritten as:

$$\Phi(z_{i-1/2}) = \frac{x_i}{\exp(Pe_m h_{i-1}) - 1} - \frac{x_{i-1}}{1 - \exp(-Pe_m h_{i-1})} + O(h_{i-1}^2). \quad \text{(A4)}$$

A similar expression can be obtained for $\Phi(z_{i+1/2})$. Integrating Eq. 4 between $z_{i-1/2}$ to $z_{i+1/2}$ gives:

$$\int_{z_{i-1/2}}^{z_{i+1/2}} \left[ \frac{1}{Le} \frac{\partial x}{\partial t} + M(x - x_p) \right] dz = \Phi(z_{i+1/2}) - \Phi(z_{i-1/2}). \quad \text{(A5)}$$

Using central rectangular representation of the integral and backward difference for the time derivative we obtain:

$$\frac{1}{Le} \frac{x_{ij} - x_{i,j-1}}{\Delta t_j} + M(x_{ij} - x_{pij}) = \frac{2}{(h_{i-1} + h_i)} [\Phi(z_{i+1/2,j}) - \Phi(z_{i-1/2,j})] + O[\max(h_i)], \quad \text{(A6)}$$

which yields Eq. 15.

Similarly we can write:

$$\left( x - \frac{1}{Pe_m} \frac{\partial x}{\partial z} \right)_{z=0} = -\Phi(z_{1/2,j}) + O(h_0) = \frac{x_{0j}}{[1 - \exp(-Pe_m h_0)]} - \frac{x_{1j}}{[\exp(Pe_m h_0) - 1]} + O(h_0), \quad \text{(A7)}$$

which gives Eq. 16.

It can be proven that the numerical scheme is absolutely stable and that the solution satisfies the integral balance.

## Appendix 2: Parameter Values for Figures 6-10 and 13

We report here a set of actual parameters which gives rise to the dimensionless parameter values used in Figures 6-10 and 13.

$C_f = 0.1$ (kmol·m$^{-3}$), $c_f = 400$ (J·kg$^{-1}$·K$^{-1}$),
$c_s = 1.9 \times 10^3$ (J·kg$^{-1}$·K$^{-1}$), $D = 10^{-3}$ (m$^2$·s$^{-1}$),
$E = = 10^8$ (J·kmol$^{-1}$),
$E_a = 1.5 \times 10^7$ (J·kmol$^{-1}$), $E_d = 5 \times 10^7$ (J·kmol$^{-1}$),
$h = 10^3$ (J·m$^{-2}$·s$^{-1}$·K$^{-1}$), $h_w = 60$ (J·m$^{-2}$·s$^{-1}$·K$^{-1}$),
$k(T_r) = 0.2$ (s$^{-1}$), $k_a(T_r) = 4.8 \times 10^{-8}$ (m·s$^{-1}$),
$k_d(T_r) = 2.4 \times 10^{-10}$ (kmol·m$^{-2}$·s$^{-1}$), $k_c = 0.05$ (m·s$^{-1}$),
$L = 1$ (m), $Q_s = 7 \times 10^{-8}$ (kmol·m$^{-2}$),
$r = 1.5 \times 10^{-2}$ (m), $r_p = 2.5 \times 10^{-3}$ (m),
$S_g = 2 \times 10^5$ (m$^2$·kg$^{-1}$), $T_r = 600$ (K), $T_w = 520$ (K),
$u = 0.2$ (m·s$^{-1}$), $(-\Delta H) = 1.2 \times 10^8$ (J·kmol$^{-1}$),
$(-\Delta H_a) = 3.4 \times 10^8$ (J·kmol$^{-1}$), $\epsilon = 0.4$,
$\lambda = 80$ (J·m$^{-1}$·s$^{-1}$·K$^{-1}$), $\rho_f = 50$ (kg·m$^{-3}$),
$\rho_s = 700$ (kg·m$^{-3}$).

*Manuscript received Apr. 23, 1992, and revision received July 7, 1992.*